Eur. Phys. J. Appl. Phys. (2016) 74: 24604
DOI: 10.1051/epjap/2015150336

THE EUROPEAN PHYSICAL JOURNAL APPLIED PHYSICS

Regular Article

Copper:molybdenum sub-oxide blend as transparent conductive electrode (TCE) indium free*

Mehdi Hssein[1,a], Linda Cattin[2], Mustapha Morsli[3], Mohammed Addou[1], and Jean-Christian Bernède[4]

[1] LOPCM, Université Ibn Tofail, Faculté des Sciences, BP 133, 14000 Kenitra, Morocco
[2] Université de Nantes, Institut des Matériaux Jean Rouxel (IMN), CNRS, UMR 6502, 2 rue de la Houssinière, BP 92208, 44000 Nantes, France
[3] Université de Nantes, Dpt Physique, 2 rue de la Houssinière, BP 92208, 44000 Nantes, France
[4] Université de Nantes, MOLTECH-Anjou, CNRS, UMR 6200, 2 rue de la Houssinière, BP 92208, 44000 Nantes, France

Received: 3 July 2015 / Received in final form: 23 September 2015 / Accepted: 2 October 2015
Published online: 3 May 2016 –

Abstract. Oxide/metal/oxide structures have been shown to be promising alternatives to ITO. In such structures, in order to decrease the high light reflection of the metal film it is embedded between two metal oxides dielectric. MoO_{3-x} is often used as oxide due to its capacity to be a performing anode buffer layer in organic solar cells, while silver is the metal the most often used [1]. Some attempts to use cheaper metal such as copper have been done. However it was shown that Cu diffuses strongly into MoO_{3-x} [2]. Here we used this property to grow simple new transparent conductive oxide (TCE), i.e., Cu: MoO_{3-x} blend. After the deposition of a thin Cu layer, a film of MoO_{3-x} is deposited by sublimation. An XPS study shows more than 50% of Cu is present at the surface of the structure. In order to limit the Cu diffusion an ultra-thin Al layer is deposited onto MoO_{3-x}. Then, in order to obtain a good hole collecting contact with the electron donor of the organic solar cells, a second MoO_{3-x} layer is deposited. After optimization of the thickness of the different layers, the optimum structure is as follow:

$$\text{Cu (12 nm) : } MoO_{3-x} \text{ (20 nm)/Al (0.5 nm)/} MoO_{3-x} \text{ (10 nm).}$$

The sheet resistance of this structure is $R_{sq} = 5.2\ \Omega$/sq. and its transmittance is $T_{max} = 65\%$. The factor of merit $\Phi_M = T^{10}/R_{sq.} = 2.41 \times 10^{-3}\ \Omega^{-1}$, which made this new TCE promising as anode in organic solar cells.

1 Introduction

Recently the interest in organic optoelectronic devices raised steadily owing to their interesting properties, such as low cost, mechanical flexibility, small weight. Indium tin oxide (ITO) is widely used as transparent anode in these devices [1].

ITO is the most often used as TCE because it presents many advantages such as excellent optical properties (large transmittance in the visible region and large bandgap), good conductivity, and high work function. However, it has also some disadvantages such as indium scarcity, aggressive techniques of deposits for organic materials and brittleness.

To date, there is an increasing demand for flexible optoelectronic devices, achieved on plastic and the brittleness of ITO makes it incompatible with flexible plastic substrates. Therefore, there is a rising demand for alternative TCEs. Numerous alternative TCEs have been explored in order to avoid the use of ITO.

The idea that comes first to mind to realize electrodes without indium is to replace the ITO by another TCO. Zinc oxide (ZnO) and tin oxides (SnO_2) are well known. For these materials several reviews were already published [2,3]. If standard deposition procedures for these films allow TCE electrical and optical requirements to be achieved routinely, the techniques used for their deposition, sputtering, pulsed laser deposition, are as aggressive as those used for ITO, while their flexibility is as limited as that of ITO.

Beside other TCO, conducting polymers [4,5], metal grid embedded in polymer [6,7], carbon nanotubes [8–10], grapheme [11,12], metal nanowires [13–16], semitransparent metal electrodes [17–20] and multilayers structures

[a] e-mail: hss.mehdi@gmail.com

* Contribution to the topical issue "Materials for Energy Harvesting, Conversion and Storage (ICOME 2015) – Elected submissions", edited by Jean-Michel Nunzi, Rachid Bennacer and Mohammed El Ganaoui

have been proposed [1,21,22]. If, up to now, these alternatives do not have all the potential of ITO, some of them have already the potential to answer the prerequisites for specific applications. In the field of vacuum deposition, in order to avoid sputtering, TCE can be obtained using evaporation or sublimation of metals and different oxides/dielectrics.

Therefore, an alternative solution is the use of semitransparent thin metal films. These layers have received renewed interest because of their higher flexibility than that of the TCOs, what makes them potential candidates for deposition on plastic substrates. Moreover, the new concept of bilayer thin metal films is also being investigated due to their higher performances than those of equivalent single layer structures [17–20].

The idea of multilayer structures is carried at its peak by the realization and the study of the structures oxide/metal/oxide (O/M/O).

The deposition of semitransparent thin metal films is easier than the realization of the O/M/O, which requires the sequential deposition of layers whose thickness is well controlled. However, it is difficult to reach a good compromise that allow for transparent and conductive layers. In fact when the layers are conductive, i.e., continue, they strongly reflect light. Therefore, the introduction of dielectric layers of high refractive index n is required so as to reduce the reflexivity of the electrodes while maintaining their conductivity. In the present work we show that a good compromise can be obtained between these two techniques by using adapted materials.

In the O/M/O multilayers structures MoO_{3-x} is often used as oxide due to its capacity to be a performing anode buffer layer in organic solar cells, while silver is the metal the most often used [1,22]. Some attempts to use cheaper metal such as copper have been done. However it was shown that Cu diffuses strongly into MoO_{3-x} [23]. Here we used this property to grow simple TCE, i.e., Cu:MoO_{3-x} blend. The study of the electrical and optical properties of this blend shows that it exhibits promising properties for its use as alternative TCE.

2 Experimental

After cleaning the glass substrate were loaded in the vacuum chamber (10^{-5} Pa). The Cu and MoO_{3-x} were deposited by simple sequential joule effect sublimation (MoO_3) or evaporation (Cu). The different layers were deposited onto substrates at room temperature. The deposition rate and thickness were measured in-situ with a quartz monitor, with the help of a rotating mask.

The optical measurements were carried out at room temperature using a Perkin spectrophotometer. The optical transmission was measured in the 0.3–1.2 μm spectral range. The four-probe technique was used to measure the electrical conductivity.

The surface topography and the cross section of the structures were observed with a field emission scanning electron microscope (SEM, JEOL F-7600). The SEM operating voltage was 5 kV. In order to improve the visualization of the cross section, images in secondary (SEM) and backscattering (BEI) mode were done.

XPS measurements were carried out at room temperature. An Axis Nova instrument from Kratos Analytical spectrometer with Al Kα line (1486.6 eV) as excitation source has been used. The core level spectra were acquired with an energy step of 0.1 eV and using a constant pass energy mode of 20 eV (energy resolution of 0.48 eV). Concerning the calibration, binding energy of the C 1s hydrocarbon peak was set at 284.8 eV. The pressure in the analysis chamber was maintained lower than 10^{-7} Pa. The background spectra are considered as Shirley type.

The quantitative study of the films was based on the determination of the Mo $3d_{5/2}$ and Cu $2p_{3/2}$, peak areas with 1.726 and 3.547 as relative sensitivity factors (RSF) respectively.

3 Experimental results and discussion

Following a preliminary review of the literature [1,22] we have initially fixed the Cu thickness to 11 nm and we studied the influence of the thickness of the MoO_{3-x} layer on the optical properties of the structures (structures Cu (11 nm)/MoO_{3-x} (x nm). The optimal thickness of the MoO_{3-x} bottom layer in O/M/O structure being 20 nm [24], we limit the maximum MoO_{3-x} layer thickness to this value. Then we fixed the MoO_{3-x} thickness to the optimum thickness experimentally determined and we used the Cu layer thickness (t_{Cu}) as parameter (9.5 nm $<$ t_{Cu} $<$ 14.5 nm) (structures Cu (x nm)/MoO_{3-x} (20 nm)).

Knowing that Cu diffuse strongly into MoO_{3-x} and that a very thin Al layer allows limiting this diffusion [23], we also realized structures Cu (x nm)/MoO_{3-x} (20 nm)/Al (1 nm)/MoO_{3-x} (10 nm). This last configuration made these structures directly usable as an anode in organic optoelectronic devices.

3.1 Optical and electrical characterization

The transmission curves of the structures Cu (11 nm)/MoO_{3-x} (x nm), with x = 10, 15, 20 nm are presented in Figure 1a. Not only has the transmittance maximum increased with the MoO_{3-x} thickness but also the width of the transmission spectrum. As said above, and in order to preserve the conductivity of the structures, we limited the MoO_{3-x} thickness to 20 nm. Then we studied the influence of the Cu thickness.

The transmission curves of the structures Cu (x nm)/MoO_{3-x} (20 nm) are presented in Figure 1b. It can be seen that, by comparison with Cu alone, the MoO_{3-x} layer allows improving significantly the transmission of the structures. The transmission increases with the Cu thickness from 9.5 nm to 12 nm and then it decreases. If the maximum value of the transmission is only 73%, the width of the transmission spectrum is very broad, broader than that usually encountered using O/M/O structures [1].

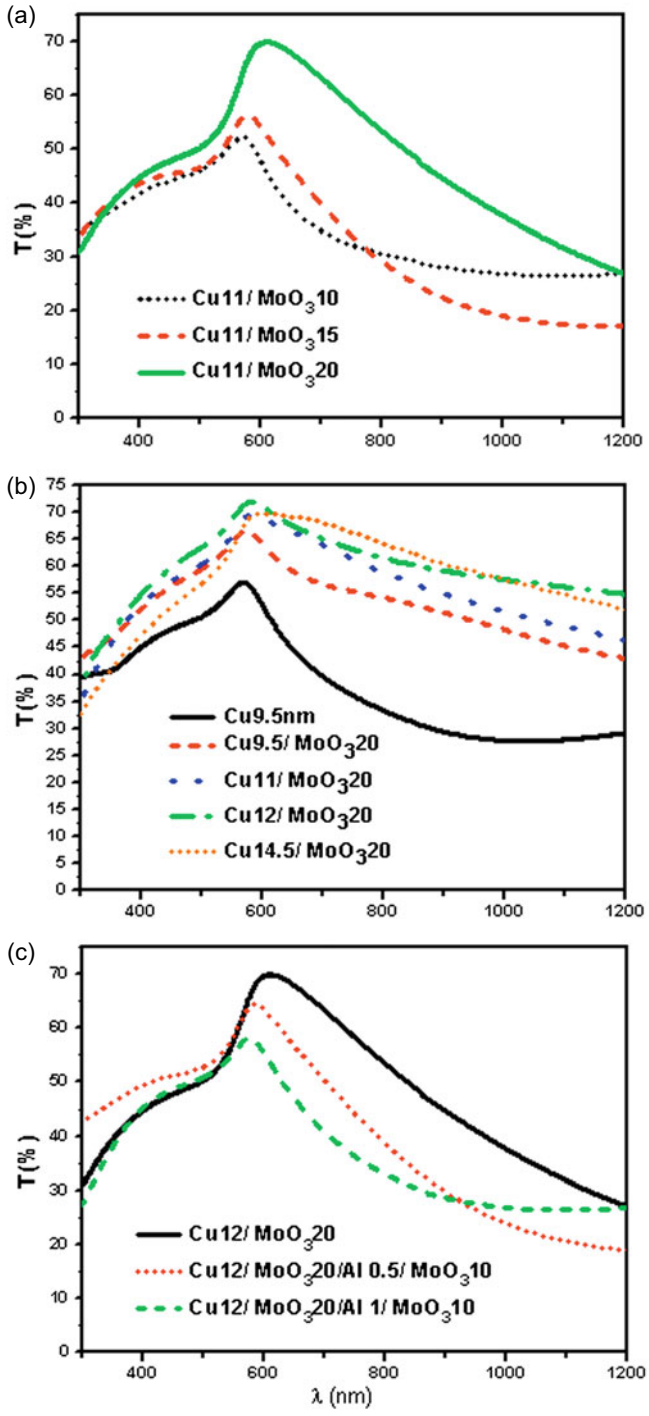

Fig. 1. Transmittance spectra of the glass/Cu/MoO_{3-x} with different layer thickness.

Starting with these optimum structures we proceeded to the realization of structures Cu (12 nm)/MoO_{3-x} (20 nm)/Al (x nm)/MoO_{3-x} (10 nm). The transmission curves obtained with $x_{Al} = 0$, 0.5 and 1 nm are shown in Figure 1c. It can be seen that, even for 0.5 nm, the Al layer induces a slight decrease of the transmission, decay increasing with the Al thickness.

After studying the optical transmission of the structures we proceed to the electrical characterization of the most promising structures.

It is interesting to note that, for a Cu thickness given, the structure which exhibits the best transmission curve gives the better sheet resistance. For instance, when a Cu layer thick of 11 nm is used, the best sheet resistance, 90 Ω/sq., is obtained for the structure Cu (11 nm)/MoO_{3-x} (20 nm). If this value is promising it remains lower than those obtained with the O/M/O structures.

Therefore, as discussed above, in order to limit the Cu diffusion and to improve the electrical properties of the structures, we introduced an Al ultra thin layer. If, as shown in Figure 1c, the transmittance is slightly decreased, the conductivity of the structures is notably augmented. For instance, in the case of a structure Cu (12 nm)/MoO_{3-x} (20 nm)/Al (0.5 nm)/MoO_{3-x} (10 nm) the sheet resistance is 5.2 Ω/sq., which is a very small and promising value. That of MoO_3 alone is around 10^6 Ω/sq.

Therefore in order to measure the real potentialities of this structure we use the classification technique proposed by Haacke [25].

The factor of merit Φ_M proposed by Haacke is $\Phi_M = T^{10}/R_{sq}$, with T transmission and R_{sq} the sheet resistance of the structure. The factor of merit Φ_M calculated for the best structure, i.e., Cu (12 nm)/MoO_{3-x} (20 nm)/Al (0.5 nm)/MoO_{3-x} (10 nm) is $\Phi_M = 2.41 \times 10^{-3}$ Ω^{-1}. This value is higher than that achieved with MoO_3/Al/Cu/Al/MoO_3 (0.43×10^{-3} Ω^{-1} [23]) and of the same order of magnitude than that achieved by MoO_3/Ag/MoO_3 (1.3×10^{-3} Ω^{-1}).

In order to better understand the different behaviors of the structures we proceeded to some physico-chemical characterization.

3.2 Physico-chemical characterization of the different structures

The Figure 2 shows the images of the surface of typical Cu (12 nm)/MoO_{3-x} (20 nm) (Fig. 2a) and Cu (12 nm)/MoO_{3-x} (20 nm)/Al (0.5 nm)/MoO_{3-x} (10 nm) (Fig. 2b) structures. There is no significant difference visible. The surface layer is very homogeneous and granular, with an averaged grain size around 100 nm.

Since Cu diffuses in MoO_{3-x} it is important to check if this diffusion is homogeneous. So we used the backscattering mode to perform some images. In that mode, the heavier atoms appear brighter on the photos. Cu being heavier than MoO_{3-x}, if amounts of Cu are present they should be clearer than the matrix of the layer. In fact, no white grains are visible in Figure 3, which testifies that the Cu diffusion into MoO_{3-x} is homogeneous.

On the effectiveness of the ultra-thin Al layer as Cu blocking layer, we proceeded to the visualization of the cross section of structure with and without Al intermediate layer. It can be seen in Figure 4 that the profiles depend on the structure.

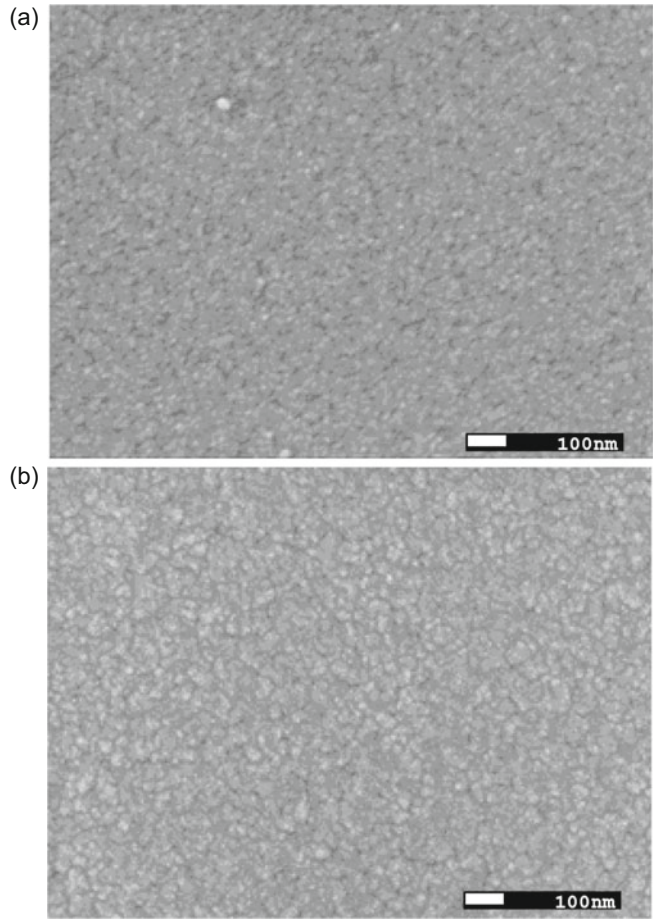

Fig. 2. Scanning electron microphotography showing the surface morphology of (a) Cu (12 nm)/MoO_{3-x} (20 nm) and (b) Cu (12 nm)/MoO_{3-x} (20 nm)/Al (0.5 nm)/MoO_{3-x} (10 nm).

In Figure 4a, the cross section of a structure Cu/MoO_{3-x}/Al/MoO_{3-x} is visualized using the backscattering mode. The backscattering mode allows discriminating two zones with different brightness.

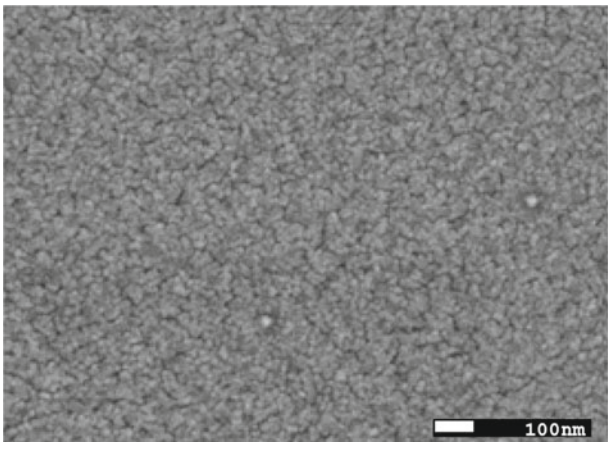

Fig. 3. SEM visualization of the surface of glass/Cu/MoO_{3-x} in the backscattering mode.

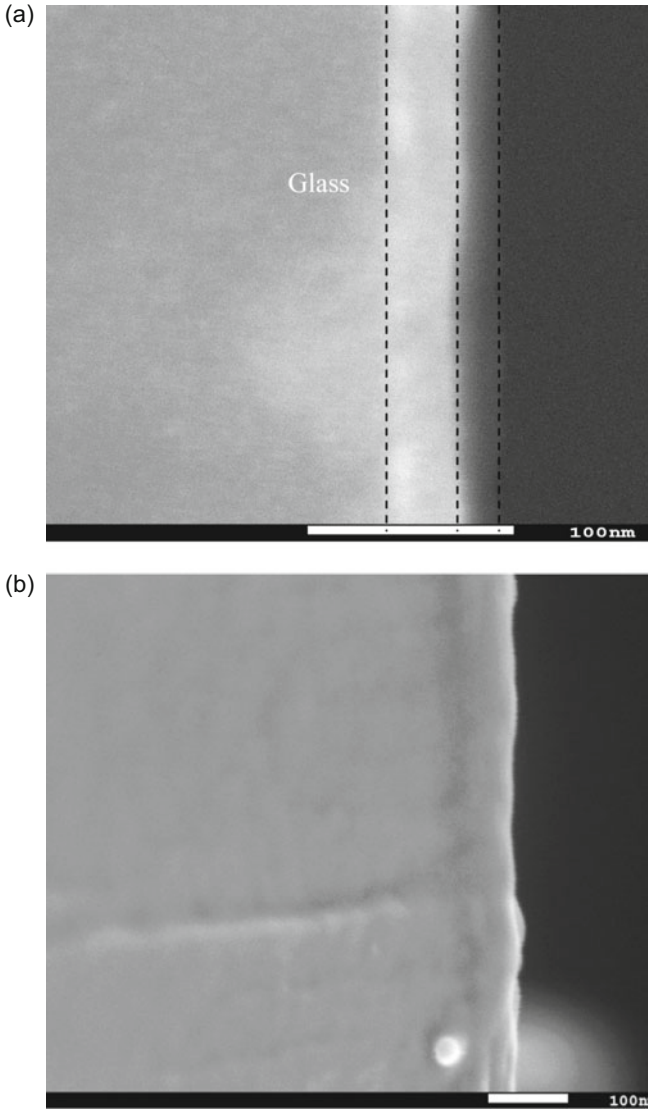

Fig. 4. Cross section visualization of Cu/MoO_{3-x}/Al/MoO_{3-x} (a) and Cu/MoO_{3-x} (b).

The bottom layer is brighter than the upper layer. It is due to the presence of higher density of quite heavy Cu atoms into that layer, than in the upper layer. Such layer differentiation is not present in the case of simple Cu/MoO_{3-x} structures (Fig. 4b). That means that Al has some effectiveness in blocking Cu atoms. However we note the presence of more bright spots near the glass substrate, reflecting a residual inhomogeneous diffusion of Cu, attesting that the Al layer is not continuous because of its very small thickness. This relative effectiveness was checked by XPS analysis. A quantitative analysis of the surface of the structures shows that in the case of Cu/MoO_{3-x}, we have 40 at.% of Mo for 60 at.% of Cu. In the case of Cu/MoO_{3-x}/Al/MoO_{3-x}, the thickness of the Al ultra thin layer being 0.5 nm, there are only 40 at.% of Cu.

The XPS spectra for a Cu/MoO_{3-x} structures are presented in Figure 5. The Mo 3d signal corresponds to two doublets (Fig. 5b). The main Mo $3d_{5/2}$ peak is situated

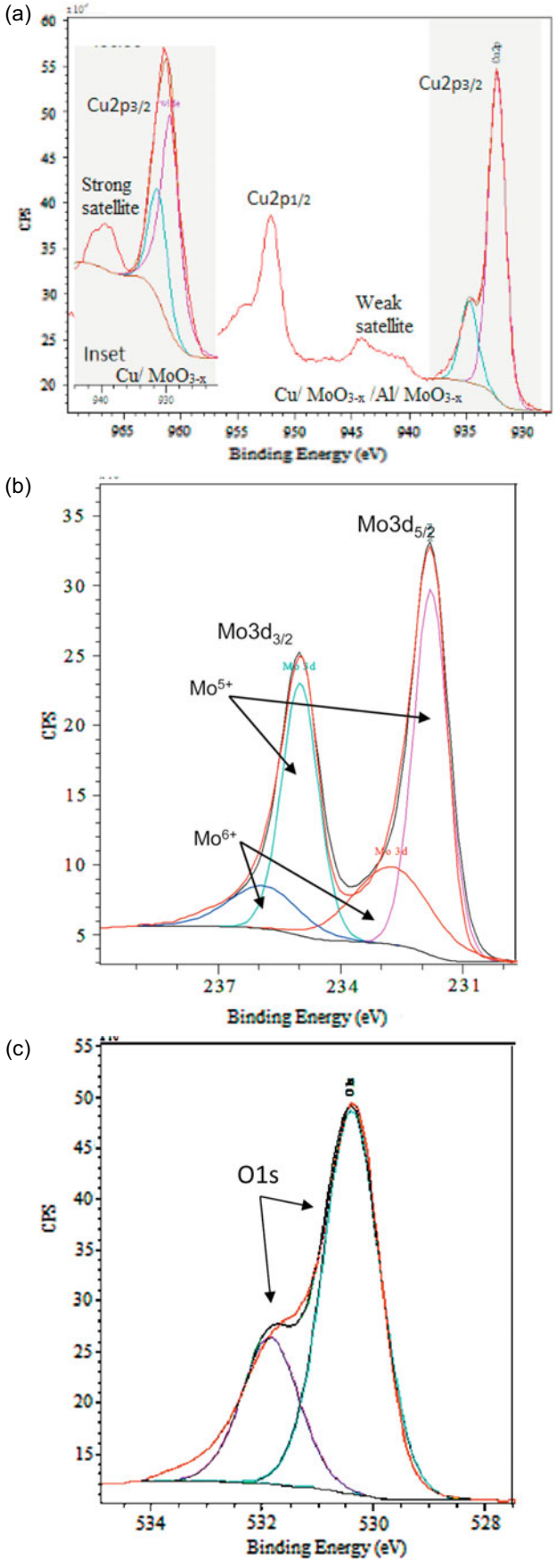

Fig. 5. XPS spectrum of Cu 2p (a), Mo 3d (b) and O 1s (c).

at 231.8 eV, the second one is situated at 232.7 eV. Therefore, the main peak can be attributed to Mo^{5+}, while the second one corresponds to Mo^{6+} [26]. It is known that MoO_{3-x} deposited by sublimation under vacuum is oxygen deficient. In our case, the atomic composition of a MoO_{3-x} film thick of 50 nm was checked by microprobe analysis.

The atomic composition measured corresponds to $MoO_{2.6}$, which explains the presence of Mo^{5+} and also the easiness of Cu to diffuse into MoO_{3-x}. The O 1s peak (Fig. 5c) corresponds to two contributions. The main one situated at 530.4 eV corresponds to oxygen bounded to a metal such as Mo and Cu [27], the second one, at 531.85 eV corresponds to some surface contamination. The shape of the Cu 2p doublet in Figure 5a is typical of a partly oxidized copper layer. Actually, it is known that the oxidation not only induces a shift of the Cu 2p doublet, but also modifies strongly the shape of the curve [28]. A decomposition of the Cu $2p_{3/2}$ peak allows estimating that around 30% of Cu is oxidized in the case of Cu/MoO_{3-x} (inset Fig. 3a) and 15% in the other case.

4 Conclusions

New transparent conductive electrode exempt of indium with a factor of merit $\Phi_M = 2.41 \times 10^{-3}\ \Omega^{-1}$ was achieved using a very simple technique. Due to spontaneous Cu diffusion into MoO_{3-x}, a simple sequential deposition Cu/MoO_{3-x} allows to obtain a conductive layer. After optimisation of the thickness of the different layers we show that it is possible to improve the performances of these structures by adding on their top a new sequential deposition Al/MoO_{3-x}. Actually the Al ultra thin layer (0.5 nm) allows to limit the Cu diffusion and therefore to improve the conductivity and the stability of the electrode.

This work was financially supported by the CNRST (PP Ministère, Morocco). Authors are grateful to N. Stephant (IMN) for his technical assistance in scanning electron microscopy.

References

1. L. Cattin, J.C. Bernède, M. Morsli, Phys. Status Solidi A **210**, 1047 (2013)
2. C.G. Granqvist, Sol. Energy Mater. Sol. Cells **91**, 1529 (2007)
3. A.E. Delahoy, S. Guo, in *Handbook of Photovoltaic Science and Engineering*, edited by A. Luque, S. Hegedus (John Wiley & Sons, Ltd., New York, 2011), pp. 716–795
4. C.-K. Cho, W.-J. Hwang, K. Eun, S.-H. Choa, S.-I. Na, H.-K. Kim, Sol. Energy Mater. Sol. Cells **95**, 3269 (2011)
5. M. Manceau, D. Angmo, M. Jorgensen, F.C. Krebs, Org. Electr. **12**, 566 (2011)
6. N. Espinosa, R. Garcia-Valverde, A. Urbina, F. Lenzmann, M. Manceau, D. Angmo, F.C. Krebs, Sol. Energy Mater. Sol. Cells **97**, 3 (2012)

7. M.L. Machana, L. Mueller-Meskamp, S. Gang, S. Olthof, K. Leo, Org. Electr. **12**, 1518 (2011)
8. A. Moujoud, S.H. Oh, H.S. Shin, H.J. Kim, Phys. Status Solidi A **207**, 1704 (2010)
9. R.J. Peh, Y. Lu, F. Zhao, C.-L. Ken Lee, W.L. Kwan, Sol. Energy Mater. Sol. Cells **95**, 3579 (2011)
10. T.H. Lim, K.W. Oh, S.H. Kim, Sol. Energy Mater. Solar-Cells **101**, 232 (2012)
11. R. Po, C. Carbonera, A. Bernardi, F. Tinti, N. Camaioni, Sol. Energy Mater. Sol. Cells **100**, 97 (2012)
12. A. Kasry, M. El Ashry, R.A. Nistor, A.A. Bol, G.S. Tulevski, G.J. Martyna, D.M. News, Thin Solid Films **520**, 4827 (2012)
13. S. Pang, Y. Hernandez, X. Feng, K. Müllen, Adv. Mater. **23**, 2779 (2011)
14. Y. Wang, S.W. Tong, X.F. Xu, B.Ö. Zyilaz, K.P. Loh, Adv. Mater. **23**, 1514 (2011)
15. F. Torrisi, T. Hasan, W. Wu, Z. Sun, A. Lombardo, T.S. Kulmala, G.-W. Hsieh, S. Jung, F. Bonaccorso, P.J. Paul, D. Chu, A.C. Ferrari, Condens. Matter Mater Sci. **21**, 11 (2011)
16. J.-Y. Lee, S.T. Connor, Y. Cui, P. Peumans, Nano Lett. **8**, 689 (2008)
17. S.D. Yambem, K.-S. Liao, S.A. Corran, Sol. Energy Mater. Sol. Cells **95**, 3060 (2011)
18. N. Formica, D.S. Ghosh, T.L. Chen, C. Eickhoff, I. Bruder, V. Pruneri, Sol. Energy Mater. Sol. Cells **107**, 63 (2012)
19. N. Formica, D.S. Ghosh, T.L. Chen, J. Hwang, C. Eickhoff, V. Pruneri, Sol. Energy Mater. Sol. Cells **116**, 89 (2013)
20. D.S. Ghosh, N. Formica, A. Carrilero, T.L. Chen, R.E. Simpson, V. Pruneri, ACS Appl. Mater. Interfaces **5**, 3048 (2013)
21. K. Ellmer, Nature Photon. **6**, 809 (2012)
22. C. Guillén, J. Herrero, Thins Solid Films **520**, 1 (2011)
23. I. Pérez Lopéz, L. Cattin, D.-T. Nguyen, M. Morsli, J.C. Bernède, Thin Solid Films **520**, 6419 (2012)
24. D.-T. Nguyen, S. Vedraine, L. Cattin, P. Torchio, M. Morsli, F. Flory, J.C. Bernède, J. Appl. Phys. **112**, 063505 (2012)
25. G. Haacke, J. Appl. Phys. **47**, 4086 1976
26. J.C. Bernède, L. Cattin, M. Morsli, Technol. Lett. **1**, 5 (2014)
27. `http://srdata.nist.gov/xps/EngElmSrchQuery.aspx?EType=PE&CSOpt=Retri_ex_dat&Elm=O`
28. N. Pauly, S. Tougaard, F. Yubero, Surf. Sci. **620**, 17 (2014)